Contents lists available at SciVerse ScienceDirect

Materials Letters

A bifunctional TiO$_2$ sol for convenient low-temperature fabrication of dye-sensitized solar cells

Wei Chen, Yangqiao Liu *, Jianqiang Luo, Jing Sun *, Lian Gao

State Key Lab of High Performance Ceramics and Superfine Microstructures, Shanghai Institute of Ceramics, Chinese Academy of Sciences, 1295 Ding Xi Road, Shanghai 200050, People's Republic of China

ARTICLE INFO

ABSTRACT

A TiO$_2$ sol was synthesized and acted as a precursor of TiO$_2$ nanoparticles in the application of low temperature dye-sensitized solar cells. It can also be used as an interparticle binder in the TiO$_2$ mesoprous films. The overall efficiency of the cell with sol addition was found to be 13% higher than the one without it and achieved 4.41% under irradiation of 100 mW/cm^2 AM1.5 sunlight. Electrochemical impedance spectra were applied to analyze the internal resistance changes of the cells with and without sol. Fine particles in the sol were proven to increase the electron life-time by improving the interconnectivity of the main particles.

© 2011 Elsevier B.V. All rights reserved.

1. Introduction

Dye-sensitized solar cells (DSSCs) [1] have attracted a lot of attention for almost two decades. This new generation solar cell enjoys low-cost and environmentally benign fabrication compared to Si-based photovoltaic cells. The light-to-electricity conversion efficiency of DSSCs has reached over 10% based on rigid glass substrates through high-temperature sintering [2, 3]. Substituting the glass with a plastic substrate enables roll-to-roll electrode fabrication and thus enlarges the application of DSSCs. However, due to the thermal instability of the mainly used polyethylene terephthalate (PET) or polyethylene naphthalate (PEN), high temperature (>150 °C) sintering of the electrodes cannot be applied, which causes an insufficient necking effect among TiO$_2$ nanoparticles and results in poor cell efficiency. So it is necessary to develop a method to fabricate the electrode at low temperature. Several methods have been proposed toward low-temperature fabrication of TiO$_2$ porous films such as mechanical press of nanocrystal films [4], film transfer process [5], electrophoretic deposition [6, 7], UV light irradiation [8] and chemical sintering [9]. All these methods required several steps of post treatment. Miyasaka et al. developed a simple method focusing on improving the connectivity in the films and obtained good photovoltaic performance [10]. But the large content of rutile phase TiO$_2$ in the paste is reported [11] to be disadvantageous to solar energy conversion in DSSCs. Adding titanium alkoxides in TiO$_2$ paste [12] was also proved to be effective to enhance efficiency of low-temperature DSSCs, but the paste was unstable when exposed to ambient environment, which makes the fabrication operable only under humidity-free conditions.

Recently, improved particle connection through adding fine TiO$_2$ particles, synthesized in acetic solution, into TiO$_2$ paste was achieved by Li et al. [13] Higher efficiency can be realized by substituting the multi-phase P25 particles with pure anatase ones. In this work, we synthesized a stable TiO$_2$ sol in a basic condition and it served both as an interparticle binder and a hydrothermal precursor of main particles in the TiO$_2$ films. The water-based paste was conveniently prepared by mixing the sol and the obtained TiO$_2$ suspension after hydrothermal reaction. The addition of sol in the paste was confirmed to have a positive effect on cell efficiency. To further investigate the effect of the sol, transmission electron microscopy, field emission scanning electron microscopy (FESEM) and electrochemical impedance spectra (EIS) were used to observe the nanoparticles, morphology of the photoanode and analyze the internal resistance in the solar cells, respectively.

2. Experimental

The TiO$_2$ paste was prepared through a modified method according to the reported procedure [14]. Briefly, titanium isopropoxide (TIP) in isopropanol was added to an aqueous solution containing tetramethylammonium hydroxide (TMAH) and then stirred for 1 h. The resultant colloid was refluxed at 100 °C for 4 h under stirring. After the peptization, the TiO$_2$ sol was divided into two parts, one for hydrothermal reaction at 230 °C for 6 h, while the other with no further treatment. The TiO$_2$ suspensions obtained from the hydrothermal treatment were sonicated, followed by concentrating through a rotatory evaporator. The TiO$_2$ suspensions and the TiO$_2$ sol were mixed in a weight ratio of 10:1 to get the final paste of which the particle content was set to ~12.5 wt.%. The TiO$_2$ suspensions were also diluted with deionized water to have the same particle content, but no addition of sol, for comparison.

* Corresponding authors. Tel.: +86 21 52412722; fax: +86 21 52413122.
E-mail addresses: yqliu@mail.sic.ac.cn (Y. Liu), jingsun@mail.sic.ac.cn (J. Sun).

The TiO$_2$ films were coated on FTO glasses using a doctor-blading method. After drying at room temperature, the films were heated at 150 °C for 1 h, followed by immersing the electrodes into 0.5 mM solution of N719 in mixed acetonitrile and t-butanol (1:1 vol) at 60 °C for 12 h for dye loading. A mixture of 0.12 M I$_2$, 0.1 M LiI and 0.5 M tert-butylpyridine in 3-methoxypropionitrile was used as the electrolyte. A sputtered Pt glass served as the counter electrode. A 0.1 cm^2 sized sandwich-type cell was simply assembled with no sealing using binder clips.

The morphology of the samples was observed through transmission electron microscopy (JEM-2100F, JEOL, Tokyo, Japan) and field emission scanning electron microscopy (FESEM, JSM-6700F, JEOL, Tokyo, Japan) was used to determine the microstructure of the TiO$_2$ films. Phase identification was done by the powder X-ray diffraction, using Rigaku X-ray diffractometer. Photocurrent–voltage measurements were performed under AM1.5 100 mW/cm^2 simulated light irradiation (YSS-80A, Japan) using a Xe lamp as the light source equipped with an infrared (IR) filter. Electrochemical Impedance Spectra (EIS) measurements were carried out with an electrochemical analyzer (CHI660C, CHI, USA). Dye loading of the TiO$_2$ films was determined by soaking sensitized electrodes in 0.1 M NaOH aqueous solution and measuring with ultraviolet–visible (UV–vis) spectrometer (Lambda 950, Perkin Elmer Co., Shelton, USA).

3. Results and discussion

Several groups have used TiO$_2$ precursors, such as TIP and TBOT (tetrabutoxytitanium), to improve the particle connectivity [12, 15]. The TiO$_2$ particles have to be dispersed in absolute ethanol and the paste is sensitive to the humidity of the ambient condition. The sol, used here, was stable and observed no change for more than one-month storage. It can also be prepared in large amount and kept as a stock solution which could act as the precursor and particle binder. TEM image of TiO$_2$ sol particles was illustrated in Fig. 1a. The sol particles were around 5 nm size, and were confirmed to be anatase by powder XRD diffraction pattern (Fig. 1b).

Compared to sintered TiO$_2$ nanocrystalline films, low temperature fabricated photoanode is lack of interparticle connection [16], namely the necking among particles. Fine particles in TiO$_2$ sol served as a binder, which could increase the interconnectivity among TiO$_2$ nanoparticles. Fig. 1c–f shows the surface morphologies of the TiO$_2$ films
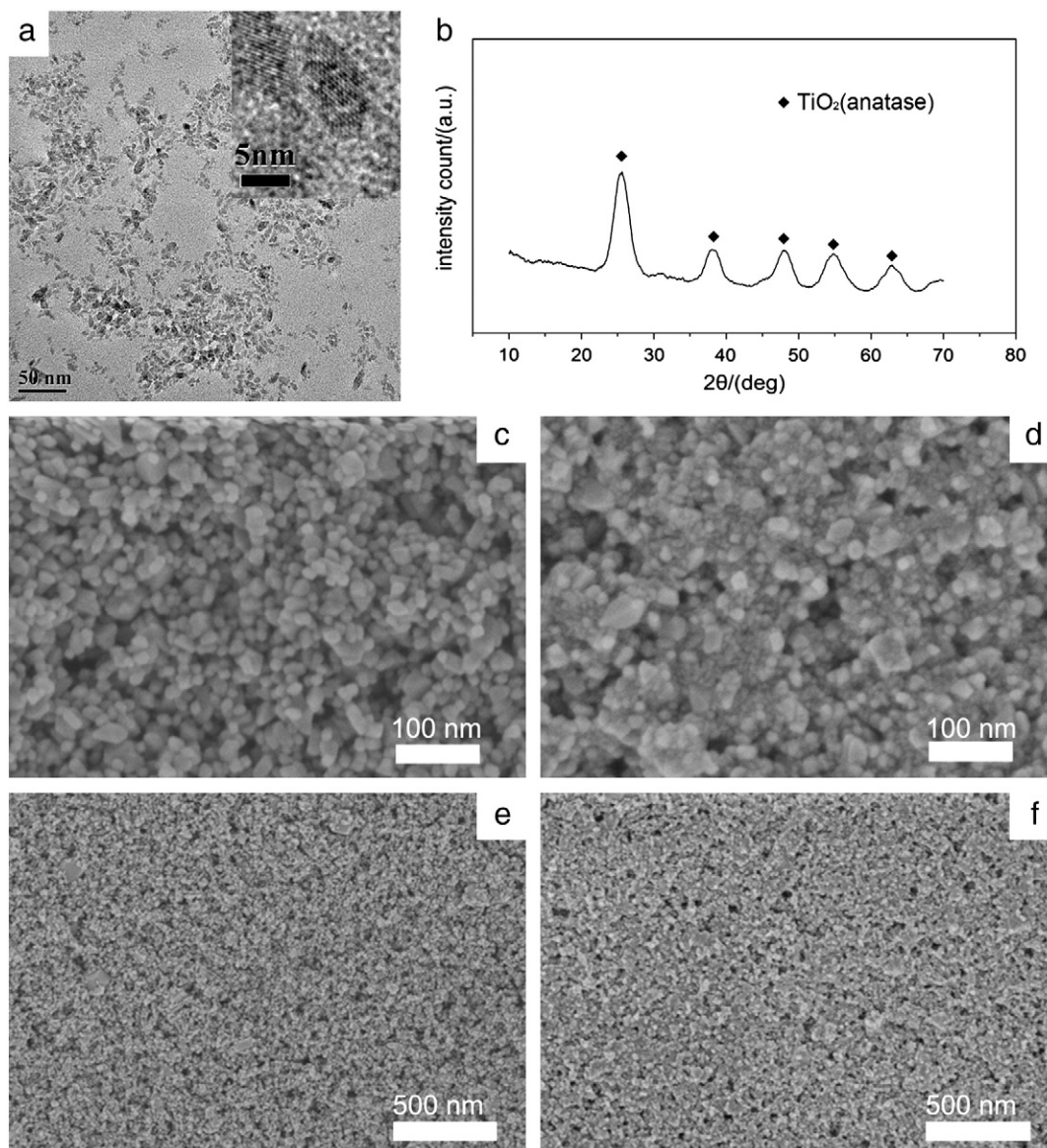

Fig. 1. (a) TEM micrograph of TiO$_2$ sol particles; the inset shows the magnified image of sol particles. (b) XRD diffraction pattern of TiO$_2$ sol particles. FESEM micrograph of TiO$_2$ films without (c), (e) and with (d), (f) addition of TiO$_2$ sol.

examined by a field emission scanning electron microscope (FESEM). As seen in Fig. 1c, the size of most particles in the film is around 20 nm, while some larger particles exist due to the growth of colloids in basic hydrothermal condition [17]. From Fig. 1d, it can be noticed that main particles are well connected by fine particles with the addition of sol. It is supposed that sol particles were homogeneously dispersed in the paste and then anchored to the TiO_2 nanoparticles through forming oxolation in films during dehydration at 150°C, which established good electron transportation path. By comparing the two films at lower magnification (Fig. 1e,f), we found that due to the pore-filling effect of fine particles, the pores in film containing sol are smaller than the one without sol.

Photocurrent–voltage characterization of cells with these two different films is shown in Fig. 2. The resultant photovoltaic parameters and dye loading are summarized in Table 1. The cell with and without sol achieved overall efficiency of 4.41% and 3.87%, respectively. The 13% increase of efficiency was mainly ascribed to the rise of J_{sc}, as a result of interparticle connection improvement and increased dye loading by addition of sol.

For further understanding the role of the sol particles in the film, we carried out electrochemical impedance spectra (EIS) measurements under illumination at a bias potential of V_{oc}. Fig. 3 shows the impedance spectra of TiO_2 films with and without sol. The addition of the sol shifts the mid-frequency peak (1–100 Hz) in the Bode phase plot (Fig. 3a) to lower frequencies. As the location of the mid-frequency peak is inverse to the effective electron lifetime [18], it suggests that electron lifetime was increased owing to faster transportation paths paved by the sol particles. In Nyquist plot, the width of the arc observed in intermediate-frequency region (R_{TiO_2}) is correlated to the electron transport resistance (R_t) in TiO_2 and recombination resistance (R_{rec}) at TiO_2/electrolyte interface. Generally, for a film with fast electron transport, R_t is manifested as a short straight line at higher frequencies due to electron diffusion [19]. Contrast to this, for a film with insufficient necking, the linear feature will become more obvious as a result of relatively large R_t. By comparing the shape of mid-frequency arcs of these two films in Fig. 3b, we can observe that the film without sol addition shows more linear feature at higher frequencies, which means a larger R_t resulting from poor connectivity. In addition, higher dye loading of sol-addition film leads to smaller R_{rec} as higher local concentration of I_3^- is produced by additional regeneration process.

According to the dye loading measurement and EIS results, it can be concluded that TiO_2 sol particles in the film have three effects: (1) interparticle connectivity improvement through binder effect; (2) enhanced dye adsorption due to higher surface area; (3) increasing local concentration of I_3^- in mesoporous film. All these three effects contributed to the performance of the cells. Though the increased I_3^- is expected to accelerate the recapture of conduction band electrons, the
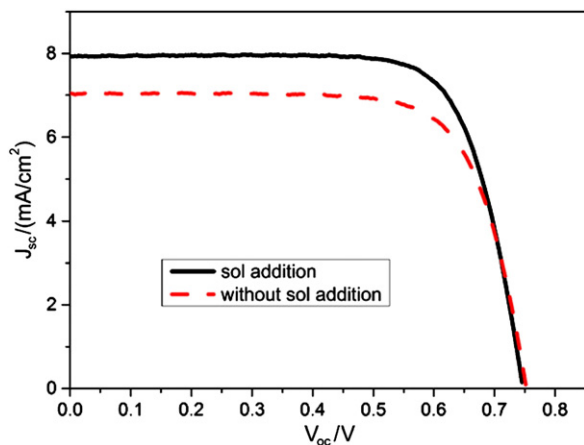
Table 1
Performance and dye loading of DSSCs based on TiO_2 films with and without sol addition.

DSSC	J_{sc} (mA/cm^2)	V_{oc} (V)	FF (%)	η (%)	Dye loading ($\times 10^{-8}$ mol cm^{-2})
Without sol addition	7.03	0.753	73.07	3.87	5.54
Sol addition	7.93	0.747	74.34	4.41	6.08

improved connectivity and dye loading compensated it and then raised the overall efficiency of the cell. On the other hand, fine particles may also fill the area that was not covered by the main particles at FTO/TiO_2 interface and then enhance the interaction between films and substrates.

4. Conclusion

In summary, we synthesized a TiO_2 sol in a basic environment and applied it as an interparticle binder in the TiO_2 nanocrystalline film as well as a hydrothermal precursor for main larger particles. The low-temperature fabricated solar cell on FTO glass achieved an overall efficiency of 4.4%, which was 13% higher than the one without sol addition. Through comparing EIS measurements and dye loading of the two cells, we found that the sol particles increased not only the dye loading but also the connectivity among TiO_2 larger particles. The pore size reducing effect of the fine particles should not be neglected, which could be optimized by controlling the content of sol. Higher efficiency can be achieved by further adjustment of the structure of the photoanode, such as light scattering layer.

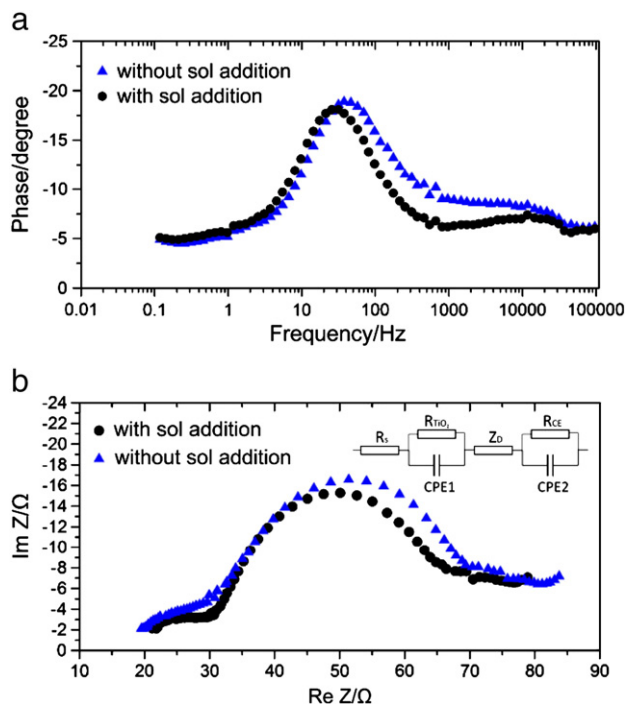**Fig. 2.** J–V curves of DSSCs based on TiO_2 films with and without addition of sol.

Fig. 3. Impedance spectra of cell with and without sol addition measured at Voc under 1 sun. (a) Bode-phase plot; (b) Nyquist plot; inset: the equivalent circuit of DSSCs. $RTiO_2$ is the electron transport resistance in TiO_2 and charge transfer resistance at TiO_2/electrolyte interface. Z_D is the diffusion resistance of electrolyte. R_{CE} is the charge transfer resistance at counter electrode/electrolyte interface. R_s is the ohmic series resistance of the cell.

References

[1] O'Regan B, Grätzel M. A low-cost, high-efficiency solar cell based on dye-sensitized colloidal TiO$_2$ films. Nature 1991;353:737–40.

[2] Ito S, Murakami T, Comte P, Liska P, Gratzel C, Nazeeruddin M, et al. Fabrication of thin film dye sensitized solar cells with solar to electric power conversion efficiency over 10%. Thin Solid Films 2008;516:4613–9.

[3] Sauvage Frédéric, Chen Dehong, Comte Pascal, Huang Fuzhi, Heiniger Leo-Philipp, Cheng Yi-Bing, et al. Dye-sensitized solar cells employing a single film of mesoporous TiO$_2$ beads achieve power conversion efficiencies over 10%. ACS Nano 2010;4:4420–5.

[4] Lindstrom Henrik, Holmberg Anna, Magnusson Eva, Lindquist Sten-Eric, Malmqvist Lennart, Hagfeldt A. A new method for manufacturing nanostructured electrodes on plastic substrates. Nano Lett 2001;1:97–100.

[5] Dürr M, Schmid A, Obermaier M, Rosselli S, Yasuda A, Nelles G. Low-temperature fabrication of dye-sensitized solar cells by transfer of composite porous layers. Nat Mater 2005;4:607–11.

[6] Miyasaka T, Kijitori Y, Murakami TN, Kimura M, Uegusa S. Efficient nonsintering type dye-sensitized photocells based on electrophoretically deposited TiO$_2$ Layers. Chem Lett 2002:1250–1.

[7] Grinis L, Kotlyar S, Rühle S, Grinblat J, Zaban A. Conformal nano-sized inorganic coatings on mesoporous TiO$_2$ films for low-temperature dye-sensitized solar cell fabrication. Adv Funct Mater 2010;20:282–8.

[8] Murakami T. Low temperature preparation of mesoporous TiO$_2$ films for efficient dye-sensitized photoelectrode by chemical vapor deposition combined with UV light irradiation. J Photochem Photobiol A Chem 2004;164:187–91.

[9] Park N-G, Kim KM, Kang MG, Ryu KS, Chang SH, Shin Y-J. Chemical sintering of nanoparticles: a methodology for low-temperature fabrication of dye-sensitized TiO$_2$ film. Adv Mater 2005;17:2349–53.

[10] Miyasaka T, Ikegami M, Kijitori Y. Photovoltaic performance of plastic dye-sensitized electrodes prepared by low-temperature binder-free coating of mesoscopic titania. J Electrochem Soc 2007;154:A455.

[11] Park N-G, van de Lagemaat J, Frank AJ. Comparison of dye-sensitized rutile- and anatase-based TiO$_2$ solar cells. J Phys Chem B 2000;104:8989–94.

[12] Fan K, Peng T, Chen J, Dai K. Effects of tetrabutoxytitanium on photoelectrochemical properties of plastic-based TiO$_2$ film electrodes for flexible dye-sensitized solar cells. J Power Sources 2011;196:2939–44.

[13] Li Y, Lee W, Lee D-K, Kim K, Park N-G, Ko MJ. Pure anatase TiO$_2$ "nanoglue": an inorganic binding agent to improve nanoparticle interconnections in the low-temperature sintering of dye-sensitized solar cells. Appl Phys Lett 2011;98:103301.

[14] Burnside SD, Shklover V, Barbé C, Comte P, Arendse F, Brooks K, et al. Self-organization of TiO$_2$ nanoparticles in thin films. Chem Mater 1998;10:2419–25.

[15] Zhang D, Yoshida T, Oekermann T, Furuta K, Minoura H. Room-temperature synthesis of porous nanoparticulate TiO$_2$ films for flexible dye-sensitized solar cells. Adv Funct Mater 2006;16:1228–34.

[16] Miyasaka T. Toward printable sensitized mesoscopic solar cells: light-harvesting management with thin TiO$_2$ films. J Phys Chem Lett 2011;2:262–9.

[17] Barbé CJ, Arendse F, Comte P, Jirousek M, Frank Lenzmann, Shklover V,, et al. Nanocrystalline titanium oxide electrodes for photovoltaic applications. J Am Ceram Soc 1997;80:3157–71.

[18] Kern R, Sastrawan R, Ferber J, Stangl R, Luther J. Modeling and interpretation of electrical impedance spectra of dye solar cells operated under open-circuit conditions. Electrochimi Acta 2002:47.

[19] Wang Q, Moser J-E, Grätzel M. Electrochemical impedance spectroscopic analysis of dye-sensitized solar cells. J Phys Chem B 2005;109:14,945–53.